IJE TRANSACTIONS A: Basics Vol. 25, No. 3, (July 2012) 289-299

International Journal of Engineering

Journal Homepage: www.ije.ir

A Simple Approach to Static Analysis of Tall Buildings with a Combined Tube-in-tube and Outrigger-belt Truss System Subjected to Lateral Loading

M. R. Jahanshahi [a], R. Rahgozar [a,*], M. Malekinejad [a,b]

[a] *Department of Civil Engineering, Shahid Bahonar University of Kerman, Kerman, Iran,*
[b] *Young Researchers Society, Shahid Bahonar University of Kerman, Kerman, Iran*

ARTICLE INFO

Article history:
Received 12 February 2012
Received in revised form 19, March, 2012
Accepted 19 April 2012

Keywords:
Tube-in-tube
Outrigger-Belt Truss
Equivalent Continuum Model
Shear Lag
Stress Functions
Displacement Functions

ABSTRACT

In this paper, an efficient technique is presented for static analysis of tall buildings with combined tube-in-tube and outrigger-belt truss system while considering shear lag effects. In the process of replacing the discrete structure with an elastically equivalent continuous one, the structure is modeled as two parallel cantilevered flexural-shear beams that are constrained at the outrigger-belt truss location by a rotational spring. Based on the principle of minimum total potential energy, simple closed form solutions are derived for stress and displacement distributions. Standard load cases, including uniformly distributed loads, triangularly distributed loads and point loads at top of the structure are considered. Results obtained from the proposed method for 50 and 60 story tall buildings are compared to those obtained using a standard finite element computer package. The approximate analyses are found to yield reasonable results and give a fairly good indication of actual structure's response..

doi: *10.5829/idosi.ije.2012.25.03a.10*

1. INTRODUCTION

Today tall buildings are seen in cities all over the world. Tubular structures have been successfully utilized and are becoming a common feature in tall buildings. Basic forms of tubular systems are the framed tube, core tube, tube-in-tube and bundled tube. A tube-in-tube structure comprises of a peripheral framed tube and a core tube interconnected by floor slabs. For each of these vertical components, various simplified models have been developed that analyze structure's behavior under lateral loads. Approximate techniques for a single tube and multi-tube systems have been developed by many researchers over the past decades. Chang analyzed tube-in-tube structures using a continuum approach in which the two beams are individually modeled by a tubular beam that accounts for flexural deformation, shear deformation, and shear lag effects [1]. Takabatake et al. [4] developed an analytical method, suitable for preliminary stages of design, and applied it to doubly symmetric tube structures in high-rise building by means of an extended rod theory that accounts for bending, transverse shear deformation, shear lag and torsion [2]. Xin et al. presented a semi-discrete displacement-based variational method to analyze tube-in-tube structures, in which framed tubes are replaced with equivalent continuous orthotropic tubes by considering shear lag effects [3]. Takabatake [4] proposed a finite difference based technique suitable for the preliminary design stages of doubly symmetric single and double frame-tubes with braces. Lee et al. [5] proposed an analytical method for modeling the discrete tube structure with multiple internal tubes in obtaining deflection and stress distributions of the structure. In this model, stress field for each member of the structure is expressed in terms of linear functions dependent on member's second moment of area, material property and geometry of the structure. Shape functions are assumed to describe displacements in flange and web frame panels for each tube [5]. Marsono and Wee studied the ultimate failure behavior of an overall reinforced concrete tube-in-tube tall building using a non-linear model [6].

The exterior and interior columns of a tube-in-tube structure are placed so closely together that they not only appear to be solid, but they act as a solid surface as well. The entire building acts as a huge hollow tube

*Corresponding Author Email: *rahgozar@mail.uk.ac.ir* (R. Rahgozar)

with a smaller tube in the middle of it. Lateral loads are shared between the inner and outer tubes. For structures may not rely on tube-in-tube interaction to resist lateral loads, girders are pin-connected to the columns, resulting a substantial increase in stiffness and subsequent decrease in lateral drift, smoothening of stress distribution in columns is obtained by tying the exterior columns of outer tube to the core tube at one or several levels with one or two story stiff horizontal outrigger trusses [7, 8].

The outrigger-braced system is regarded as one of the most effective ways of increasing structural stiffness in tall buildings and has been widely studied over the past decades [9-14]. Taranath discussed the optimum locations for a two-outrigger system [15]. Gao investigated the effect of lintel beams in the outer tube, on elastic response of the outrigger structures [16]. Fu proposed the design criteria for reinforced concrete tall building structures with outriggers [17]. Wu and Lee presented detailed analyses on how the top drift, base moment in the core and fundamental vibration period are influenced by variations in outrigger location and structural stiffness when a multi-level outrigger-braced tall building structure is subjected to uniformly distributed forces or triangularly distributed loads along the building height [18].

Recently, static and dynamic analyses of combined system of outrigger-belt truss and shear core with single tube have been studied by Rahgozar et al. and Malekinejad and Rahgozar [19, 20]. In these works framed tube structure is modeled with four orthotropic membranes [21]. The effect of shear core and outrigger-belt truss on framed tube system under lateral loads is modeled as a rotational spring at outrigger-belt truss location [15].

Most studies up to now have concentrated on static and dynamic analysis of tube-in-tube structures. Therefore work needs to be done on analysis of combined systems of tube-in-tube and outrigger-belt truss. Based on previous studies, in particular the method developed previously by Rahgozar et al. [19, 22], this paper presents detailed analysis of displacement and stress distribution functions in a combined system of tube-in-tube and multi-level outrigger-belt truss in a tall building structure that is subjected to uniformly distributed, triangularly distributed and concentrated loading along its building height considering shear lag effects.

2. SYSTEM DESCRIPTION AND ASSUMPTIONS

The design principle is to create two parallel hollow cantilevered box beams above ground that are constrained at outrigger-belt truss location by a rotational spring; as a result, the lateral loads are mainly or completely resisted by facades of the cantilever [19, 21]. Assumptions which are considered in this paper are same as those implemented by Kwan and Rahgozar et al. [19, 21]. Using continuous model, outer and inner tubes are comprised of two panels parallel to lateral load direction (web panels) and two panels perpendicular to lateral load direction (flange panels). The beams are forced to have equal lateral deflections, and the amount of load carried by each beam is a function of its relative stiffness [1]. Due to shear lag, plane sections will no longer remain plane after the structure is loaded. Herein, based on work which is carried out by Kwan [21], independent distributions for the axial displacements in the web and flange panels is made. The axial displacement distributions are assumed to be cubic in the web panels and parabolic in the flange panels and the principle of minimum total potential energy is employed for the formulation. Axial deformation in flange and web panels of outer and inner tubes are as follows:

$$w_{we} = \phi\, a \left[(1-\alpha)\frac{x}{a} + \alpha(\frac{x}{a})^3 \right] \quad (1)$$

$$w_{wi} = \phi\, a' \left[(1-\alpha')\frac{x}{a'} + \alpha'(\frac{x}{a'})^3 \right] \quad (2)$$

$$w_{fe} = \phi\, a \left[(1-\beta) + \beta(\frac{y}{b})^2 \right] \quad (3)$$

$$w_{fi} = \phi\, a' \left[(1-\beta') + \beta'(\frac{y}{b'})^2 \right] \quad (4)$$

In which subscripts e and i are used for outer and inner tubes, respectively. w_{we}, w_{wi}, w_{fe} and w_{fi} are axial deformation of outer and inner tube's webs and flanges, respectively. α, β, α' and β' are shear lag coefficients of outer and inner tube's webs and flanges, respectively. Also, a, b, a' and b' parameters are dimensions of outer and inner tubes' panels as shown in Figure 1. The x, y direction coordinates are also shown in Figure 1 and z direction coordinate is along the structure's height.

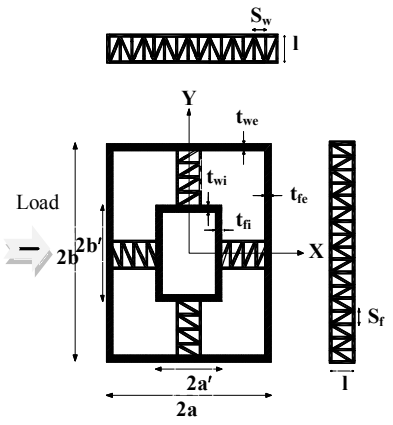

Figure 1. Tube-in-tube structure's plan at outrigger-belt truss location.

Due to axial and shear strain of outer and inner tubes, the elastic strain energy of the tube-in-tube structure can be expressed as follows:

$$\Pi_e = \int_0^H \int_{-a'}^{a'} t'_{wi} (E_{wi}\varepsilon_{zi}^2 + G_{wi}\gamma_{xzi}^2)\, dx\, dz + \int_0^H \int_{-b'}^{b'} t'_{fi} (E_{wi}\varepsilon_{zi}^2 + G_{wi}\gamma_{yzi}^2)\, dy\, dz + \int_0^H \int_{-a}^{a} t_{we} (E_{we}\varepsilon_{ze}^2 + G_{we}\gamma_{xze}^2)\, dx\, dz + \int_0^H \int_{-b}^{b} t_{fe} (E_{we}\varepsilon_{ze}^2 + G_{we}\gamma_{yze}^2)\, dy\, dz + \int_0^H 2E_{me}A_{ke}\varepsilon_{ke}\, dz + \int_0^H 2E_{mi}A_{ki}\varepsilon_{ki}\, dz \quad (5)$$

$$\varepsilon_{ze} = \frac{\partial w_{we}}{\partial z};\quad \varepsilon_{zi} = \frac{\partial w_{wi}}{\partial z} \quad (6)$$

$$\varepsilon'_{ze} = \frac{\partial w_{fe}}{\partial z};\quad \varepsilon'_{zi} = \frac{\partial w_{fi}}{\partial z} \quad (7)$$

$$\gamma_{xze} = \frac{\partial u_e}{\partial z} + \frac{\partial w_{we}}{\partial x};\quad \gamma_{xzi} = \frac{\partial u_i}{\partial z} + \frac{\partial w_{wi}}{\partial x} \quad (8)$$

$$\gamma_{yze} = \frac{\partial w_{we}}{\partial y};\quad \gamma_{yzi} = \frac{\partial w_{wi}}{\partial y} \quad (9)$$

In Equations (6-9), ε_{ze}, ε'_{ze}, ε_{zi} and ε'_{zi} are axial strains in flange and web frames of outer and inner tubes, respectively. γ_{yze}, γ_{xze}, γ_{yzi} and γ_{xzi} are shear strains of flange and web frames of outer and inner tubes, respectively. H is structure's height as shown in Figure 2.

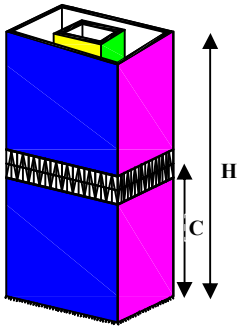

Figure 2. Equivalent tube-in-tube structure.

t_{we}, t_{fe}, t'_{wi}, t'_{fi}, E_{we}, E_{fe}, E_{wi}, E_{fi}, G_{we}, G_{fe}, G_{wi} and G_{fi} are thickness, modulus of elasticity and shear modulus of web and flange frames of outer and inner tubes, respectively.

E_{me}, E_{mi}, A_{ke}, A_{ki}, ε_{ke} and ε_{ki} are modulus of elasticity, cross sectional area and axial strain of each corner column. Potential energy of the externally applied uniform distributed load, triangular distributed load, concentrated load at top point of the structure and concentrated moment at outrigger-belt truss location are as follows [21]:

$$\Pi_{pu} = -\int_0^H U_\circ\, u(z)\, dz \quad (10)$$

$$\Pi_{pt} = -\int_0^H T\, \frac{z}{H}\, u(z)\, dz \quad (11)$$

$$\Pi_{pp} = -P\, u(H) \quad (12)$$

$$\Pi_{pM} = K\, \theta^2 \quad (13)$$

where $u(z)$ is the lateral displacement at any point along structure's height, P, U_o, T, K and θ are concentrated load at top of the structure, intensity of uniformly distributed load, maximum intensity of triangularly distributed load along height of the structure, equivalent stiffness of the rotational spring at outrigger-belt truss location, and rotation at outrigger-belt truss location, respectively.

Minimizing total potential energy of the structure with respect to parameter ϕ, describing structure's rotation distribution, yields [21]:

$$M = EI\frac{\partial \phi}{\partial z} \quad (14)$$

where EI and M are the flexural stiffness and the moment due to external loadings. In order to simplify the calculation procedure, EI can be assumed constant along structure's height [21]; hence, parameter ϕ can be expressed as follows:

$$\phi = \frac{1}{EI}\int_0^z M\, dz \quad (15)$$

In a similar manner, total potential energy of the structure is minimized with respect to unknown parameter u, yielding the governing equation in terms of u as [21]:

$$S = 4\,(G_{we}\, t_{we}\, b + G_{wi}\, t_{wi}\, b')\,(\frac{\partial u}{\partial z} + \phi) \quad (16)$$

Hence, u can be expressed as [21]:

$$u = \int_0^z \left(\frac{S}{4\,(G_{we}\, t_{we}\, b + G_{wi}\, t_{wi}\, b')} - \phi \right) dz \quad (17)$$

where S is the shear related to external loads.

3. SHEAR LAG PARAMETERS

Substituting ϕ and u from Equations (15) and (17) into the total potential energy statement of the structure and minimizing it with respect to unknown shear lag coefficients, the governing equations for α and β can be obtained. For simplicity, α and β are estimated via polynomial functions with unknown coefficients α_1, α_2, β_1, β_2, α'_1, α'_2, β'_1 and β'_2. Applying boundary condition at top of the structure where axial stress is

zero gives: $d\beta/dz = d\alpha/dz = d\beta'/dz = d\alpha'/dz = 0$ and then minimizing the total potential energy with respect to parameters α_1, α_2, β_1, β_2, α_1', α_2', β_1' and β_2', yields the shear lag coefficients in web and flange panels of inner and outer tubes. Shear lag coefficients for three cases of force and concentrated moment are listed in Tables 1-4, where C is the location of outrigger-belt truss from structure's base. α_M, β_M, α_M' and β_M' are shear lag coefficients of web and flange panels for outer and inner tubes due to the moment created by outrigger-belt truss located at C.

TABLE 1. Shear lag coefficients for concentrated load at top of the structure

α_1	$\frac{7a^2E_{we}(6a^2E_{we}+7H^2G_{we})}{24a^4E_{we}+112a^2H^2E_{we}G_{we}+42H^4G^2{}_{we}}$
α_2	$\frac{7a^2E_{we}(24a^2E_{we}+7H^2G_{we})}{8(12a^4E_{we}{}^2+56a^2H^2E_{we}G_{we}+21H^4G_{we}{}^2}$
β_1	$\frac{35b^2E_{fe}(18b^2E_{fe}+5H^2G_{fe})}{504b^4E_{fe}{}^2+560b^2H^2E_{fe}G_{fe}+50H^2G_{fe}{}^2}$
β_2	$\frac{35b^2E_{fe}(72b^2E_{fe}+5H^2G_{fe})}{8(252b^2E_{fe}{}^2+280b^2H^2E_{fe}G_{fe}+25H^4G_{fe}{}^2)}$

TABLE 2. Shear lag coefficients for uniformly distributed load along structure's height

α_1	$\frac{126a^2E_{we}(53185a^2E_{we}+121947H^2G_{we})}{3.82\times10^6a^4E_{we}+1.75\times10^7a^2H^2E_{we}G_{we}+5.96\times10^6H^4G^2{}_{we}}$
α_2	$\frac{63a^2E_{we}(106370a^2E_{we}+2499H^2G_{we})}{3.82\times10^6a^4E_{we}{}^2+1.75\times10^7a^2H^2E_{we}G_{we}+5.96\times10^6H^4G_{we}{}^2}$
β_1	$\frac{810b^2E_{fe}(10637b^2E_{fe}+5807H^2G_{fe})}{6.89\times10^6b^4E_{fe}{}^2+7.52\times10^6b^2H^2E_{fe}G_{fe}+6.09\times10^5H^2G_{fe}{}^2}$
β_2	$\frac{405b^2E_{fe}(21274b^2E_{fe}+119H^2G_{fe})}{6.89\times10^6b^2E_{fe}{}^2+7.52\times10^6b^2H^2E_{fe}G_{fe}+25H^4G_{fe}{}^2}$

TABLE 3. Shear lag coefficients for triangularly distributed load along structure's height

α_1	$\frac{231a^2E_{we}(3061830a^2E_{we}+62583663H^2G_{we})}{4.04\times10^9a^4E_{we}+1.86\times10^{10}a^2H^2E_{we}G_{we}+6.54\times10^9H^4G^2{}_{we}}$
α_2	$\frac{231a^2E_{we}(153091151a^2E_{we}+1420204H^2G_{we})}{2.02\times10^9a^4E_{we}{}^2+9.30\times10^9a^2H^2E_{we}G_{we}+3.27\times10^9H^4G_{we}{}^2}$
β_1	$\frac{495b^2E_{fe}(214328114b^2E_{fe}+104306105H^2G_{fe})}{8.48\times10^{10}b^4E_{fe}{}^2+9.30\times10^{10}b^2H^2E_{fe}G_{fe}+7.78\times10^9H^4G_{fe}{}^2}$
β_2	$\frac{165b^2E_{fe}(321492171b^2E_{fe}+7101020H^2G_{fe})}{4.24\times10^9b^2E_{fe}{}^2+4.65\times10^{10}b^2H^2E_{fe}G_{fe}+3.89\times10^9H^4G_{fe}{}^2}$

TABLE 4. Shear lag coefficients for concentrated moment

α_1	$\frac{35a^2E_{we}(8a^2E_{we}-15C^2G_{we})}{160a^4E_{we}{}^2+680a^2C^2E_{we}G_{we}+273C^4G^2{}_{we}}$
α_2	$\frac{35a^2E_{we}(4a^2E_{we}+3C^2G_{we})}{160a^4E_{we}{}^2+680a^2C^2E_{we}G_{we}+273C^4G_{we}{}^2}$
β_1	$\frac{15b^2E_{fe}(56b^2E_{fe}-25C^2G_{fe})}{672b^4E_{fe}{}^2+680b^2C^2E_{fe}G_{fe}+65C^4G_{fe}{}^2}$
β_2	$\frac{30b^2E_{fe}(28b^2E_{fe}+5C^2G_{fe})}{672b^4E_{fe}{}^2+680b^2C^2E_{fe}G_{fe}+65C^4G_{fe}{}^2}$

4. GOVERNING PARAMETERS FUNCTIONS

4. 1. Parametric Stress Functions Flange and web frames' deflection functions may be calculated using shear lag coefficients that were presented earlier. In the derivation process of these functions, first, axial strain functions are calculated. Then axial strain functions are multiplied by modulus of elasticity for each panel and considering outrigger-belt truss effects, equations of axial stress distribution for the structure are obtained in terms of the elevation of outrigger-belt truss. Amount of load carried by each inner and outer tube is a function of its relative stiffness. Therefore, axial stress distribution functions of web and flange panels for inner and outer tubes can be stated as follows:

for $z>C$

$$\sigma_{we}=\left(\frac{EI_e}{EI_e+EI_i}\right)\left(E_{we}\frac{d\phi}{dz}b\left[(1-\alpha)\frac{x}{b}+\alpha(\frac{x}{b})^3\right]\right) \quad (18)$$

$$\sigma_{wi}=\left(\frac{EI_i}{EI_e+EI_i}\right)\left(E_{wi}\frac{d\phi}{dz}b'\left[(1-\alpha)\frac{x}{b'}+\alpha(\frac{x}{b'})^3\right]\right) \quad (19)$$

$$\sigma_{fe}=\left(\frac{EI_e}{EI_e+EI_i}\right)\left(E_{fe}\frac{d\phi}{dz}b\left[(1-\beta)+\beta(\frac{y}{a})^2\right]\right) \quad (20)$$

$$\sigma_{fi}=\left(\frac{EI_i}{EI_e+EI_i}\right)\left(E_{fi}\frac{d\phi}{dz}b'\left[(1-\beta')+\beta'(\frac{y}{a'})^2\right]\right) \quad (21)$$

for $z\le C$

$$\sigma_{we}=\left(\frac{EI_e}{EI_e+EI_i}\right)\left(E_{we}\frac{d\phi}{dz}b\left[(1-\alpha)a\frac{x}{b}+\alpha(\frac{x}{b})^3\right]-E_{we}\frac{K\theta}{EI_{ce}}b\left[(1-\alpha_M)\frac{x}{b}+\alpha_M(\frac{x}{b})^3\right]\right) \quad (22)$$

$$\sigma_{wi}=\left(\frac{EI_i}{EI_e+EI_i}\right)\left(E_{wi}\frac{d\phi}{dz}b'\left[(1-\alpha')a'\frac{x}{b'}+\alpha'(\frac{x}{b'})^3\right]-E_{wi}\frac{K\theta}{EI_{ce}}b'\left[(1-\alpha_M')\frac{x}{b'}+\alpha_M'(\frac{x}{b'})^3\right]\right) \quad (23)$$

$$\sigma_{fe}=\left(\frac{EI_e}{EI_e+EI_i}\right)\left(E_{fe}\frac{d\phi}{dz}b\left[(1-\beta)+\beta(\frac{y}{a})^2\right]-E_{fe}\frac{K\theta}{EI_{ce}}b\left[(1-\beta_M)+\beta_M(\frac{y}{a})^2\right]\right) \quad (24)$$

$$\sigma_{fi}=\left(\frac{EI_i}{EI_e+EI_i}\right)\left(E_{fi}\frac{d\phi}{dz}b'\left[(1-\beta')+\beta'(\frac{y}{a'})^2\right]-E_{fi}\frac{K\theta}{EI_{ce}}b'\left[(1-\beta'_M)+\beta'_M(\frac{y}{a'})^2\right]\right) \quad (25)$$

where σ_{we}, σ_{fe}, σ_{wi} and σ_{fi} are axial stress in web and flange frames for outer and inner tubes along structure's height while considering the outrigger-belt truss effects. EI_e and EI_i are flexural stiffness of outer and inner tubes, respectively.

Equations (18-25) depend on the unknown parameter $d\phi/dz$, which can be determined by placing axial stress of the framed tube into equilibrium equation of the structure using Equation (14) as follows:

$$M=EI\frac{\partial\phi}{\partial z}=\int_{-b}^{b}2t_{we}\,\sigma_{we}\,z\,dz+\int_{-a}^{a}2t_{fe}\,\sigma_{fe}\,b\,dx+4A_{ke}\,\sigma_{ke}\,b+\int_{-b'}^{b'}2t_{wi}\,\sigma_{wi}\,z\,dz+\int_{-a'}^{a'}2t_{fi}\,\sigma_{fi}\,b'\,dx+4A_{ki}\,\sigma_{ki}\,b' \quad (26)$$

where σ_{ke} and σ_{ki} are axial stress of the corner columns of outer and inner tubes, respectively. Equivalent flexural stiffness values EI_e and EI_i can be determined by equating the amount of $EI(\partial\phi/\partial z)$ from Equation (26) to each of the external moments due to the three load cases of concentrated load at top of the structure, triangularly and uniformly distributed loads along the height of the structure. EI_e and EI_i become:

$$EI_e=\frac{4}{3}E_{we}\,t_{we}\,b^3\left(1-\frac{2}{5}\alpha\right)+4E_{fe}\,t_{fe}\,b^2a\left(1-\frac{2}{3}\beta\right)+4\,E_{me}\,A_{ke}\,b^2 \quad (27)$$

$$EI_i=\frac{4}{3}E_{wi}\,t_{wi}\,b'^3\left(1-\frac{2}{5}\alpha'\right)+4E_{fi}\,t_{fi}\,b'^2a'\left(1-\frac{2}{3}\beta'\right)+4\,E_{mi}\,A_{ki}\,b'^2 \quad (28)$$

In a similar manner, equivalent stiffness due to concentrated moment can be expressed as follows:

$$EI_{ce}=\frac{4}{3}E_{we}\,t_{we}\,b^3\left(1-\frac{2}{5}\alpha_M\right)+4E_{fe}\,t_{fe}\,b^2a\left(1-\frac{2}{3}\beta_M\right)+4\,E_{me}\,A_{ke}\,b^2 \quad (29)$$

$$EI_{ci}=\frac{4}{3}E_{wi}\,t_{wi}\,b'^3\left(1-\frac{2}{5}\alpha'_M\right)+4E_{fi}\,t_{fi}\,b'^2a'\left(1-\frac{2}{3}\beta'_M\right)+4\,E_{mi}\,A_{ki}\,b'^2 \quad (30)$$

$$EI=EI_e+EI_i \quad (31)$$

$$EI_c=EI_{ce}+EI_{ci} \quad (32)$$

where EI_{ce} and EI_{ci} are equivalent flexural stiffness of outer and inner tubes, respectively.

Axial stress in the outer and inner tubes can be calculated from the amount of equivalent stiffness in outrigger-belt truss, K, and the amount of structure's rotation at outrigger-belt truss location.

4. 2. Parametric Displacement Function and Rotation Function along Structure's Height Lateral displacement functions of the structure due to each of the three types of load cases considered here (concentrated load at top of the structure, uniformly and triangularly distributed loads along the height of the structure) can be obtained by first substituting EI and EI_c from Equations (31) and (32) into Equation (15) and solving for ϕ and then calculating Equation (17) with the computed ϕ. If the rigidity factor EI, is variable along the height of the structure, calculation of ϕ and lateral displacement become complicated. Hence, EI and EI_c are assumed to be constant along the height of the structure and are equal to their values at structure's base [21]. Based on this assumption, lateral displacement functions of the structure due to lateral loads are expressed as follows:

Concentrated load at top of the structure:

for $z>C$:

$$u=\frac{P}{EI}(\frac{1}{2}Hz^2-\frac{1}{6}z^3)+\frac{P}{(4G_{we}t_{we}b+4G_{wi}t_{wi}b')}z-\left(\frac{K\theta_P}{EI_c}(Cz-\frac{C^2}{2})\right) \quad (33)$$

for $z\le C$:

$$u=\frac{P}{EI}(\frac{1}{2}Hz^2-\frac{1}{6}z^3)+\frac{P}{(4G_{we}t_{we}b+4G_{wi}t_{wi}b')}z-\left(\frac{K\theta_PC^2}{2EI_c}\right) \quad (34)$$

Uniformly distributed load along structure's height:

for $z>C$:

$$u=\frac{U_\circ}{EI}(\frac{1}{4}H^2z^2-\frac{1}{6}Hz^3+\frac{1}{24}z^4)+\frac{U_\circ}{(4G_{we}t_{we}b+4G_{wi}t_{wi}b')}\left(Hz-\frac{1}{2}z^2\right)-\left(\frac{K\theta_u}{EI_c}(Cz-\frac{C^2}{2})\right) \quad (35)$$

for $z\le C$:

$$u=\frac{U_\circ}{EI}(\frac{1}{4}H^2z^2-\frac{1}{6}Hz^3+\frac{1}{24}z^4)+\frac{U_\circ}{(4G_{we}t_{we}b+4G_{wi}t_{wi}b')}\left(Hz-\frac{1}{2}z^2\right)-\left(\frac{K\theta_uC^2}{2EI_c}\right) \quad (36)$$

Triangularly distributed load along structure's height:

for $z>C$:

$$u=\frac{T}{EI}(\frac{1}{6}H^2z^2-\frac{1}{12}Hz^3+\frac{1}{120}\frac{z^5}{H})+\frac{T}{(4G_{we}t_{we}b+4G_{wi}t_{wi}b')}\left(\frac{Hz}{2}-\frac{1}{6}\frac{z^3}{H}\right)-\left(\frac{K\theta_t}{EI_c}(Cz-\frac{C^2}{2})\right) \quad (37)$$

for $z\le C$:

$$u=\frac{T}{EI}(\frac{1}{6}H^2z^2-\frac{1}{12}Hz^3+\frac{1}{120}\frac{z^5}{H})+\frac{T}{(4G_{we}t_{we}b+4G_{wi}t_{wi}b')}\left(\frac{Hz}{2}-\frac{1}{6}\frac{z^3}{H}\right)-\left(\frac{K\theta_tC^2}{2EI_c}\right) \quad (38)$$

Relations for rotation of the combined system, θ, at outrigger-belt truss location at height C for the three loading cases can be derived by considering compatibility of deformations. Rotation for each load case becomes:

Concentrated load at top of the structure:

$$\theta_P=\frac{EI_c}{EI_c+KC}\left[\frac{P}{(4G_{we}t_{we}b+4G_{wi}t_{wi}b')}+\frac{P}{EI}\left(CH-\frac{C^2}{2}\right)\right] \quad (39)$$

Uniformly distributed load along structure's height:

$$\theta_u = \frac{EI_c}{EI_c + KC}\left[\frac{U_o}{EI}\left(\frac{1}{2}H^2C - \frac{1}{2}HC + \frac{1}{6}C^3\right) + \frac{U_o}{(4G_{we}t_{we}b + 4G_{wi}t_{wi}b')}(H - C)\right] \quad (40)$$

Triangularly distributed load along structure's height:

$$\theta_t = \frac{EI_c}{EI_c + KC}\left[\frac{T}{(4G_{we}t_{we}b + 4G_{wi}t_{wi}b')}\left(\frac{H}{2} - \frac{C^2}{2H}\right) + \frac{T}{EI}\left(\frac{1}{3}H^2C - \frac{1}{4}HC^2 + \frac{1}{24}\frac{C^4}{H}\right)\right] \quad (41)$$

Equivalent stiffness of the rotational spring at outrigger-belt truss location is given by Malekinejad and Rahgozar as follows [20, 24]:

$$K = 1/\left(\frac{C}{2b^2A_eE_{fe}} + \frac{C}{2b'^2A_iE_{fi}} + \frac{b^2}{6(EI)_e} + \frac{1}{kGAl}\right) \quad (42)$$

where A_e, A_i, k, G, A and l are sum of columns cross sectional areas of flange frames of outer and inner tubes, shear coefficient, shear modulus, sectional area of an outrigger-belt truss and height of outrigger-belt truss, respectively. $(EI)_e$ is the effective flexural stiffness of the outrigger.

5. COMPARING RESULTS OF THE PROPOSED METHOD TO SAP2000 ANALYSES

In this section, simplicity and accuracy of the proposed method are illustrated through numerical examples for 50 and 60 story reinforced concrete buildings with combined systems of tube-in-tube and outrigger-belt truss systems. Location of outrigger-belt truss is moved along the height of structure. All beams, columns and outrigger-belt truss members have constant sizes along the height of structure as $0.8\,m \times 0.8\,m$ and other geometrical dimensions are illustrated in Table 5. Also, actual and equivalent properties of the structure are listed in Table 6. The structure is subjected to three external load cases separately as follows:

Concentrated load at top of the structure:

$P = 18 \times 10^4\ kN$

Uniformly distributed load along the structure's height:

$U_o = 120\ kN/m$

Triangularly distributed load along the structure's height:

$T = 240\ kN/m$

Based on continuum model presented by Kwan [21] first, equivalent properties of the structure are calculated and then by calculating shear lag coefficients for different load cases, axial stresses in the inner and outer tubes and lateral displacement of the structure are calculated using Equations (18-25) and (33-38). Outrigger-belt truss is placed at different elevations (*H/6*, *H/4*, *H/2*, *3H/4* and *H*).

TABLE 5. Geometrical dimensions of the 50 and 60 story tall buildings

Height of story	Total height	Outer tube dimensions		Inner tube dimensions		Center to center columns distance	
$h_{(m)}$	$H_{(m)}$	$2b_{(m)}$	$2a_{(m)}$	$2b'_{(m)}$	$2a'_{(m)}$	$S_{w(m)}$	$S_{f(m)}$
3	150	30	50	10	20	2.5	2.5

TABLE 6. Actual and equivalent properties of the 50 and 60 story tall buildings

Actual elastic properties		Equivalent elastic properties					
		Web			Flange		
$E_{(GPa)}$	$G_{(GPa)}$	$E_{w(GPa)}$	$G_{w(GPa)}$	$t_{w(m)}$	$E_{f(GPa)}$	$G_{f(GPa)}$	$t_{f(m)}$
20	8	20	1.48	0.256	20	1.48	0.256

Displacement and axial stresses from the proposed method are compared with those obtained using SAP2000. Results for the three load cases are listed in Tables 7-12. Lateral displacement of the structure along its height, and axial stress in web and flange of the inner and outer tubes are shown in Figures 3-17 for 50-story tall building. Lateral displacement, and axial stress in web and flange of the inner and outer tubes of 60-story tall building are similar to those which are plotted for 50-story tall building. Therefore, these graphs are not repeated here.

The results presented here show that displacement values at top of the structure calculated via the proposed method are in good agreement with those obtained from SAP2000 analysis (differences are about 18 percent). Also, the proposed functions for stress distribution in web and flange panels of outer and inner tubes are accurate enough. For example, in 50-srory tall building when outrigger-belt truss is placed at height *H/6*, axial stresses in corner columns at structure's base are underestimated by 10-17 percent, axial stress at structure's base in middle columns is overestimated by 2-7 percent and the lateral displacement at top of the structure is underestimated by 2-12 percent for the three load cases considered here.

Estimating axial deformation in web and flange with cubic and quadratic functions based on research by Kwan [21]; equivalent stiffness for outrigger-belt trusses; assuming constant value for shear and flexural stiffness of the structure and using continuum modeling for the structure are sources of error in the proposed method when comparing to finite element analysis.

TABLE 7. Comparison between results for 50-story tall building subjected to concentrated load at top of the structure

C	Axial stress of middle columns of flange frames (MPa)			Axial stress of corner columns of flange frames (MPa)			Displacement at top of the structure (MPa)		
	SAP	proposed method	% of error	SAP	proposed method	% of error	SAP	proposed method	% of error
H/6	3.97	4.22	6	9.43	7.80	17	41.76	42.87	2
H/4	3.98	4.12	3	9.57	7.85	17	41.36	42.64	3
H/2	3.52	3.87	9	9.83	7.94	19	40.45	42.42	4
3H/4	3.27	3.77	15	9.99	7.98	20	40.10	40.52	1
H	3.13	3.73	19	10.07	8.73	13	40.83	40.32	1

TABLE 8. Comparison between results for 50-story tall building subjected to uniformly distributed load along structure's height

C	Axial stress of middle columns of flange frames (MPa)			Axial stress of corner columns of flange frames (MPa)			Displacement at top of the structure (MPa)		
	SAP	proposed method	% of error	SAP	proposed method	% of error	SAP	proposed method	% of error
H/6	1.78	1.81	1	5.85	5.05	13	17.75	19.93	12
H/4	1.65	1.76	6	6.02	5.13	14	17.65	19.68	11
H/2	1.36	1.47	8	6.25	5.26	15	17.71	19.17	8
3H/4	1.19	1.37	15	6.36	5.32	16	18.19	19.10	5
H	1.13	1.38	22	6.39	5.36	16	18.73	19.34	3

TABLE 9. Comparison between results for 50-story tall building subjected to triangularly distributed load along structure's height

C	Axial stress of middle columns of flange frames (MPa)			Axial stress of corner columns of flange frames (MPa)			Displacement at top of the structure (MPa)		
	SAP	proposed method	% of error	SAP	proposed method	% of error	SAP	proposed method	% of error
H/6	2.47	2.65	7	7.20	6.45	10	24.98	27.46	9
H/4	2.34	2.58	10	7.37	6.53	11	24.74	27.09	9
H/2	1.99	2.14	7	7.65	6.66	12	24.54	26.24	6
3H/4	1.76	2.04	15	7.79	6.75	13	25.11	26.06	3
H	1.67	2.03	21	7.85	6.47	17	25.98	24.83	4

TABLE 10. Comparison between results for 60-story tall building subjected to concentrated load at top of the structure

C	Axial stress of middle columns of flange frames (MPa)			Axial stress of corner columns of flange frames (MPa)			Displacement at top of the structure (MPa)		
	SAP	proposed method	% of error	SAP	proposed method	% of error	SAP	proposed method	% of error
H/6	3.99	4.72	18	11.02	9.12	17	58.32	60.23	3
H/4	4.12	4.93	19	11.71	9.49	18	58.14	60.04	3
H/2	4.27	5.07	18	11.84	9.55	19	56.71	59.84	5
3H/4	4.67	5.10	9	12.01	9.79	18	55.12	57.35	4
H	4.51	4.80	6	12.08	9.84	18	55.85	57.10	2

TABLE 11. Comparison between results for 60-story tall building subjected to uniformly distributed load along structure's height

C	Axial stress of middle columns of flange frames (MPa)			Axial stress of corner columns of flange frames (MPa)			Displacement at top of the structure (MPa)		
	SAP	proposed method	% of error	SAP	proposed method	% of error	SAP	proposed method	% of error
H/6	1.74	1.92	10	7.40	6.10	17	27.96	28.78	2
H/4	1.69	2.05	21	7.18	5.89	17	27.12	28.32	4
H/2	2.27	2.63	15	6.82	5.83	14	25.49	24.42	4
3H/4	2.53	2.65	4	7.15	5.91	17	28.20	24.20	14
H	2.44	2.54	4	7.24	6.10	15	31.77	25.97	18

TABLE 12. Comparison between results for 60-story tall building subjected to triangularly distributed load along structure's height

C	Axial stress of middle columns of flange frames (MPa)			Axial stress of corner columns of flange frames (MPa)			Displacement at top of the structure (MPa)		
	SAP	proposed method	% of error	SAP	proposed method	% of error	SAP	proposed method	% of error
H/6	2.34	2.85	21	8.82	7.13	19	40.10	45.12	12
H/4	2.15	2.47	14	9.04	7.25	19	39.75	44.53	12
H/2	1.69	2.04	20	9.27	7.32	21	39.47	43.41	9
3H/4	1.51	1.82	20	9.35	7.39	20	38.81	43.10	11
H	1.47	1.81	23	9.44	7.44	21	39.51	42.23	6

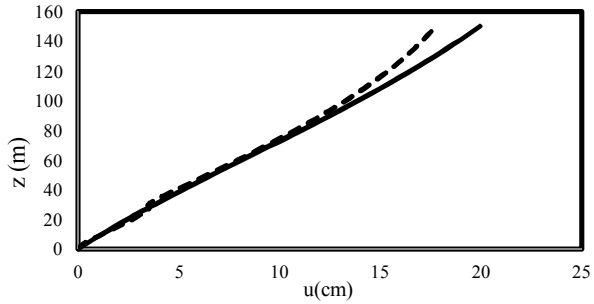

Figure 3. Displacement of 50-story combined system under uniformly distributed load along the height of structure (C = H/6).

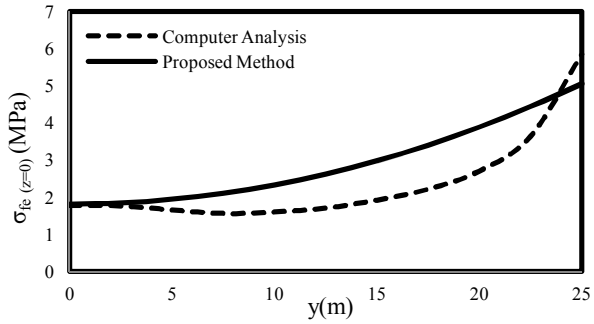

Figure 4. Axial stress distribution of half length of flange in outer tube due to distributed load along the height of 50-story tall building (C = H/6).

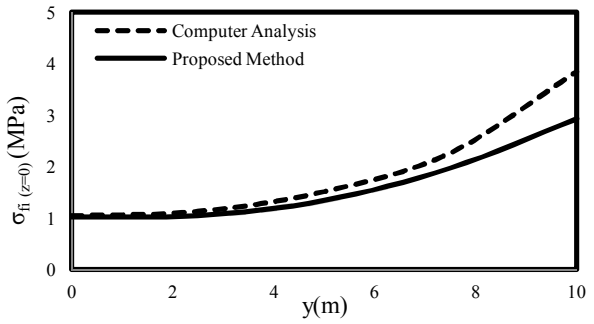

Figure 5. Axial stress distribution of half length of flange in inner tube due to distributed load along the height of 50-story tall building (C = H/6).

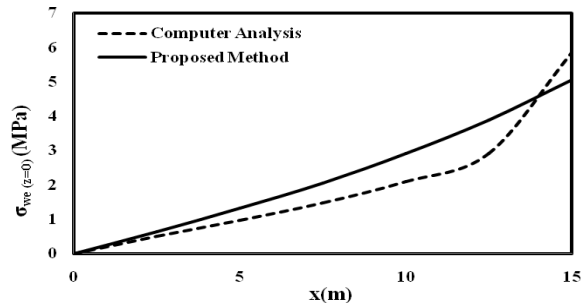

Figure 6. Axial stress distribution of half length of web in outer tube due to distributed load along the height of 50-story tall building (C = H/6).

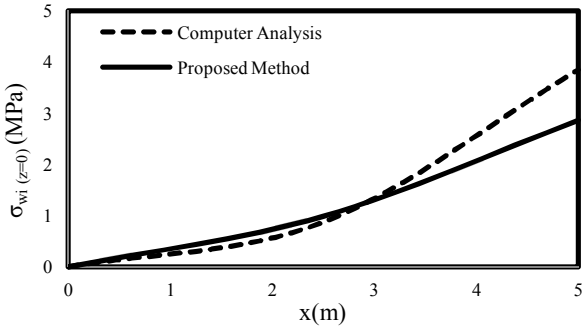

Figure 7. Axial stress distribution of half length of web in inner tube due to distributed load along the height of 50-story tall building (C = H/6).

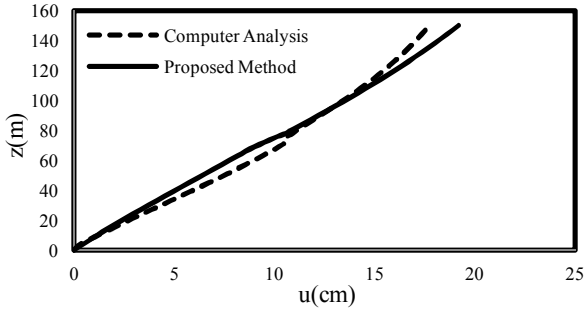

Figure 8. Displacement of 50-story combined system under uniformly distributed load along the height of structure (C = H/2).

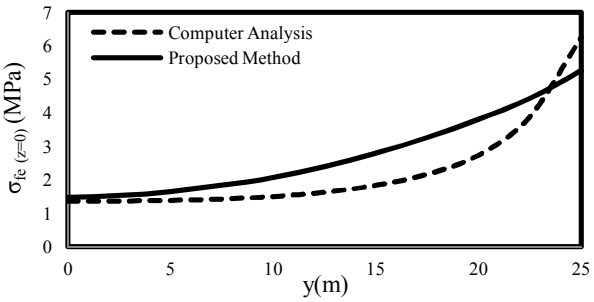

Figure 9. Axial stress distribution of half length of flange in outer tube due to distributed load along the height of 50-story tall building (C = H/2).

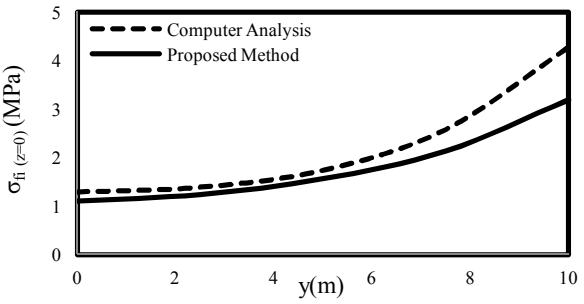

Figure 10. Axial stress distribution of half length of flange in inner tube due to distributed load along the height of 50-story tall building (C = H/2).

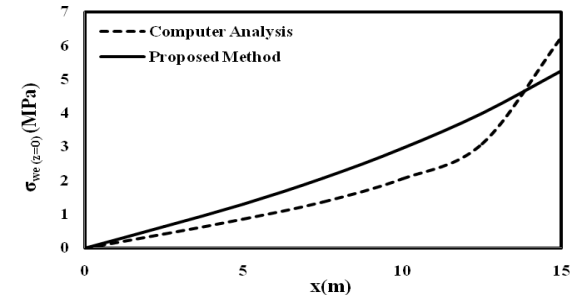

Figure 11. Axial stress distribution of half length of web in outer tube due to distributed load along the height of 50-story tall building (C = H/2).

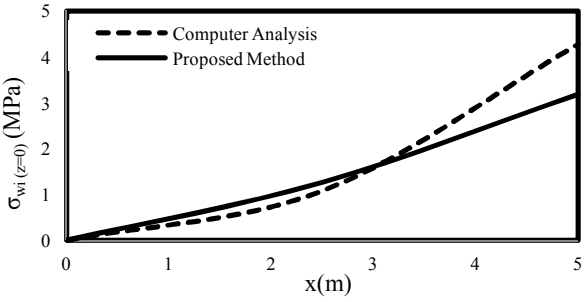

Figure 12. Axial stress distribution of half length of web in inner tube due to distributed load along the height of 50-story tall building (C = H/2).

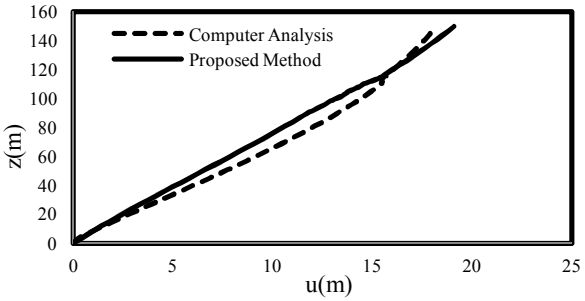

Figure 13. Displacement of 50-story combined system under uniformly distributed load along the height of structure (C = 3H/4).

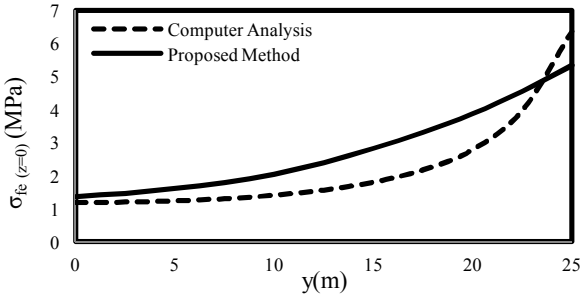

Figure 14. Axial stress distribution of half length of flange in outer tube due to distributed load along the height of 50-story tall building (C = 3H/4).

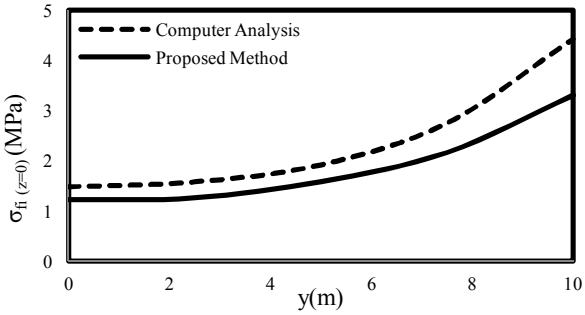

Figure 15. Axial stress distribution of half length of flange in inner tube due to distributed load along the height of 50-story tall building (C = 3H/4).

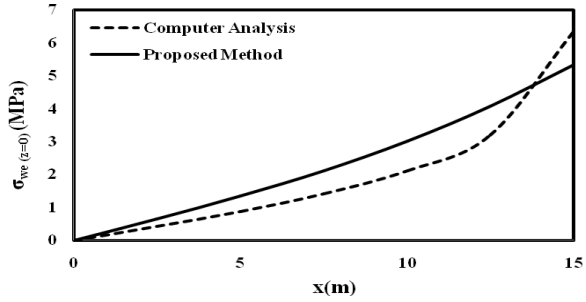

Figure 16. Axial stress distribution of half length of web in outer tube due to distributed load along the height of 50-story tall building (C = 3H/4).

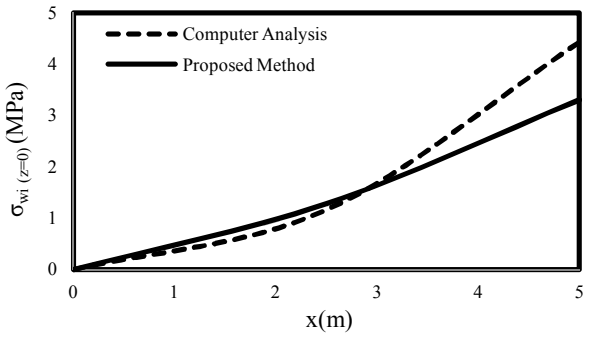

Figure 17. Axial stress distribution of half length of web in inner tube due to distributed load along the height of 50-story tall building (C = 3H/4).

6. CONCLUSSION

This paper presents parametric functions for static analysis of tall buildings with combined system of tube-in-tube and outrigger-belt truss system subjected to three separate load cases of concentrated load at top of the structure, uniformly and triangularly distributed loads along the height of the structure. Approximate formulas for estimating stress and displacement of the structure have been proposed by means of minimizing potential energy of the structure including the bending deformation; transverse shear deformation and shear lag effects in web and flange panels. The structure has been modeled by two continuous cantilever beams which are restrained at outrigger-belt truss location by a rotational spring. The formulas proposed here have been validated by comparing them to the computer static analysis results obtained from three-dimensional studies using the finite element method. It has been shown that results computed by the energy method correlate well with those obtained by means of SAP2000 analysis. Application of the method is versatile. The method is simple and the accuracy is acceptable. Also it can reduce the computational work drastically as compared to SAP2000 analysis for static analysis of combined system of tube-in-tube and outrigger-belt truss tall buildings; hence rendering it as a simple and efficient tool suitable for early stages of tall building design.

7. REFERENCES

1. Chang P. C., "Analytical modeling of tube-in-tube structure", *Journal of Structural Engineering, ASCE*, Vol. 111, No. 6, (1985), 1326-1337.
2. Takabatake H., Mukai H. and Hirano T., "Doubly symmetric tube structures, I: static analysis", *Journal of Structural Engineering*, *ASCE*, Vol. 119, No. 7, (1993), 1981–2001.
3. Xin K. G., Bao S. H. and Li W. Y., "A semi-discrete method for analysis of tube-in-tube structures", *Computer and Structures*, Vol. 53, No. 2, (1994), 319-325.
4. Takabatake H., "A simple analysis of doubly symmetric tube structures by the finite difference method", *The Structural Design of Tall and Special Buildings*, Vol. 5, (1996), 111-128.
5. Lee K. K., Loo Y. C. and Guan H., "Simple analysis of framed tube structure with multiple internal tubes", *Journal of Structural Engineering, ASCE*, Vol. 127, No. 4, (2001), 450-460.
6. Marsono A. K. and Wee L. S., "Nonlinear finite element analysis of reinforced concrete tube in tube of tall buildings", *Proceedings of the 6th Asia-Pacific Structural Engineering and Construction Conference (APSEC 2006)*, Kuala Lumpur, Malaysia (2006).
7. Taranath BS., "*Structural Analysis and Design of Tall Buildings*", McGraw Hill Book Company, New York, (1988).
8. Smith S. and Coull A., "*Tall Building Structures*", McGraw Hill Book Company, New York, (1996).
9. Taranath BS., "Optimum belt truss location for high-rise structures", *Structural Engineer*, Vol. 53, No. 8, (1975), 18–21.
10. McNabb JW. and Muvdi BB., "Drift reduction factors for belt high-rise structures", *Engineering Journal*, *AISC*, Vol. 12, No. 3, (1975), 88–91.
11. Stafford Smith B. and Salim I., "Parameter study of outrigger-braced tall building structures", *Journal of Structural Engineering, ASCE*, Vol. 107, No. 10, (1981), 2001-2014.
12. Ding JM., "Optimum belt truss location for high-rise structures and top level drift coefficient", *Journal of Building Structures*, Vol. 4, (1991), 10–13.
13. Zhu YL., "Inner force analysis of frame–core structure with horizontal outrigger belts", *Journal of Building Structures*, Vol. 10, (1995), 10–15.
14. Zhang ZG., Fu XY., Wang JJ. and Wei YN., "Studies on structural performance of ultra high-rise building with outrigger belts", *Journal of Building Structures*, Vol. 17, No. 4, (1996), 2–9.
15. Taranath BS., "*Steel, concrete, and composite design of tall buildings*", McGraw-Hill, New York, (1998).
16. Gao P., "Structural behavior of ultra high-rise building with outrigger belts", *Journal of Building Structures*, Vol. 10, (1998), 8–12.
17. Fu XY., "Design proposal for reinforced concrete high-rise building structure with outrigger belts", *Journal of Building Structures*, Vol. 10, (1999), 11–19.
18. Wu J. R. and LI Q. S., "Structural performance of multi-outrigger braced tall buildings", *The Structural Design of Tall and Special Buildings*, Vol. 12, (2003), 155–176.
19. Rahgozar R., Ahmadi R. A., Hosseini O. and Malekinejad M., "A simple mathematical model for static analysis of tall buildings with two outrigger-belt truss systems", *Structural Engineering and Mechanics*, Vol. 40, No. 1, (2011), 65-84.
20. Malekinejad M. and Rahgozar R., "Free vibration analysis of tall buildings with outrigger-belt truss system", *An International Journal of Earthquakes and Structures*, Vol. 2, No. 1, (2011), 89-107.
21. Kwan AKH., "Simple method for approximate analysis of framed tube structures", *Journal of Structural Engineering, ASCE*, Vol. 120, No. 4, (1994), 1221-1239.
22. Rahgozar R., Ahmadi A. and Sharifi Y., "A simple mathematical model for approximate analysis of tall buildings", *Journal of Applied Mathematical Modelling, Elsevier*, Vol. 34, (2010), 2437-2451.

23. Chaboki Khiabani, A., Sadrnejad, S. A. and Yahyaeii, M., "Stress transfer modeling in CNT reinforced composites using mechanics", *International Journal of Engineering*, Vol. 21, No. 3, (2008), pp. 227-234.

24. Malekinejad, M. and Rahgozar, R., "A close form solution for free vibration analysis of tube-in-tube systems in tall buildings", *International Journal of Engineering*, Vol. 25, No. 2, (2012), pp. 91-99.

A Simple Approach to Static Analysis of Tall Buildings with a Combined Tube-in-tube and Outrigger-belt Truss System Subjected to Lateral Loading

M. R. Jahanshahi [a], R. Rahgozar [a], M. Malekinejad [a,b]

[a] *Department of Civil Engineering, Shahid Bahonar University of Kerman, Kerman, Iran,*
[b] *Young Researchers Society, Shahid Bahonar University of Kerman, Kerman, Iran*

ARTICLE INFO

Article history:
Received 12 February 2012
Received in revised form 19, March, 2012
Accepted 19 April 2012

Keywords:
Tube-in-tube
Outrigger-Belt Truss
Equivalent Continuum Model
Shear Lag
Stress Functions
Displacement Functions

چکیده

در این مقاله یک روش مؤثر به منظور آنالیز استاتیکی ساختمان‌های بلند با سیستم ترکیبی قاب محیطی تو در تو و سیستم مهار بازویی و کمربند خرپایی با در نظر گرفتن اثرات لنگی برش ارائه گردیده است. در روش ارائه شده، سازه گسسته با یک سازه پیوسته الاستیک معادل جایگزین شده است که در آن، سازه توسط دو تیر طره موازی خمشی- برشی که در محل قرارگیری مهار بازویی و کمربند خرپایی به‌وسیله یک فنر پیچشی مقید شده، مدل شده است. بر اساس اصل کمینه‌سازی انرژی کل سازه، توابعی برای توزیع تنش و جابه‌جایی در ارتفاع سازه ارائه شده است. سه نوع بارگذاری استاندارد شامل بار گسترده یکنواخت، بار گسترده مثلثی و بار متمرکز در تراز فوقانی سازه در نظر گرفته شده است. نتایج به‌دست آمده با استفاده از روش پیشنهادی برای ساختمان‌های بلند ۵۰ و ۶۰ طبقه با نتایج حاصله از آنالیز کامپیوتری مقایسه شده است. روش تقریبی پیشنهادی نتایج قابل قبولی ارائه می‌دهد که به تخمین بسیار خوبی از پاسخ سازه واقعی منجر می‌گردد.

doi: *10.5829/idosi.ije.2012.25.03a.10*